Dam-break induced flow over mobile beds, numerical approach in volume of fluid method

Alireza Khoshkonesh, Ph.D. in hydraulics, water structures, department of water engineering, Bu-Ali Sina university, Hamedan 65178, (Islamic republic of Iran)
Email: alirezakhshknsh42@gmail.com
Fariba Ahmadi Dehrashid*, Ph.D. student in hydraulics, water structures, department of water engineering, Bu-Ali Sina university, Hamedan 65178, (Islamic republic of Iran)
Email: faribaahmadi91@gmail.com
Blaise NSOM, Université de Bretagne Occidentale. IRDL/UBO UMR CNRS 6027. Rue de Kergoat, 29285 Brest, France
Email: blaise.nsom@univ-brest.fr
Saeed Gohari, Assistant professor of hydraulics structures, Department of Water Engineering, Faculty of Agri-culture, Bu-Ali Sina University, Hamedan, 65178, (Islamic republic of Iran)
Email: s.gohari@basu.ac.ir
Hossein Banejad, Associate professor of hydraulics, department of water engineering, college of agriculture, Fer-dowsi university of Mashhad, Mashhad, 91735 (Islamic republic of Iran)
Email: banejad@um.ac.ir
Payam Heidarian, MSc in water and hydraulic structures engineering, Department of hydraulic structures, Faculty of civil and environment engineering, Tarbiat Modares University, Iran
Email: pym.heidarian@gmail.com

Abstract
In this paper, the effect of the sediment bed elevation on dam-break flow over mobile beds is scrutinized using the volume of fluid (VOF) method. While the equations of motion are tackled employing the finite-volume and standard k-ε turbulence closure model. The morphological characteristics are studied using the van Rijn bed load transport model. The results show that an increase in the downstream bed elevation leads to reducing: a) the flow advancing distance and water rising over the end wall, b) the sediment transport rate downstream and c) the reservoir releasing rate. It causes the formation and evolution of two hydraulic jumps and corresponding scour holes in the near field and the downstream channel.

Keywords
Dam-break, Mobile-bed, Bed elevation, k-ε, RANS, VOF.

Introduction

The ideal dam-break means the release of a still water column within a prismatic tank due to an instantaneous removal of a sluice gate. This study is of great im-portance in flood routing and controlling, coastal engineering, hazards analysis and risk management. Likewise, many dams around the world are confronted with the sedimentation inside the reservoir and downstream of the channel. Whereas, there is a significant level-difference between the sediments within the up and downstream due to the height of the dam crest (Fig. 1). In the solution, the wave-front maximum velocity is twice the surface wave celerity ($um=2c=2\sqrt{gH0}$), where um, c, g and H0 rep-resent the maximum velocity, the surface wave celerity, gravity acceleration and the still water level, re-spectively. Besides, the reservoir width and length, slope and fluid viscosity are crucial factors on free surface deformations and flow advancing distance (Stansby et al. (1998)., Nsom et al. (2000)., Nsom et al. (2007)., Nsom et al. 2019). Further, the wave front advancing distance and flow velocity over a fixed bed is higher than the mobile-bed case because of the bed resistance effects. Whereas, there is a direct rela-tionship between the reservoir initial water level and the free-surface evolution (Capart and Young, (1998)., Fraccarollo and Capart, (2002)., Spinewine (2005)., Cao et al. (2004)., Wu and Wang, (2008)., Khoshkonesh et al. (2019). Therefore, a few studies have done on the bed elevation effects on dam-break flow. The 3D models based on the Navier-Stokes equations predict the dam-break flow features with high accuracy. Further, the dynamic pressure distribution is calculated in the near filed and throughout the computational domain. In this way, the volume of fluid (VOF) method is used to track the free surface evolution. for the first time, the effect of the bed elevation is scrutinized on the free surface and bed profiles, subsequent hydraulic jumps and scour holes depths. Hence, the effect of sediment bed elevation on dam-break flow evolution is scrutinized using VOF method by Flow-3D CFD package.

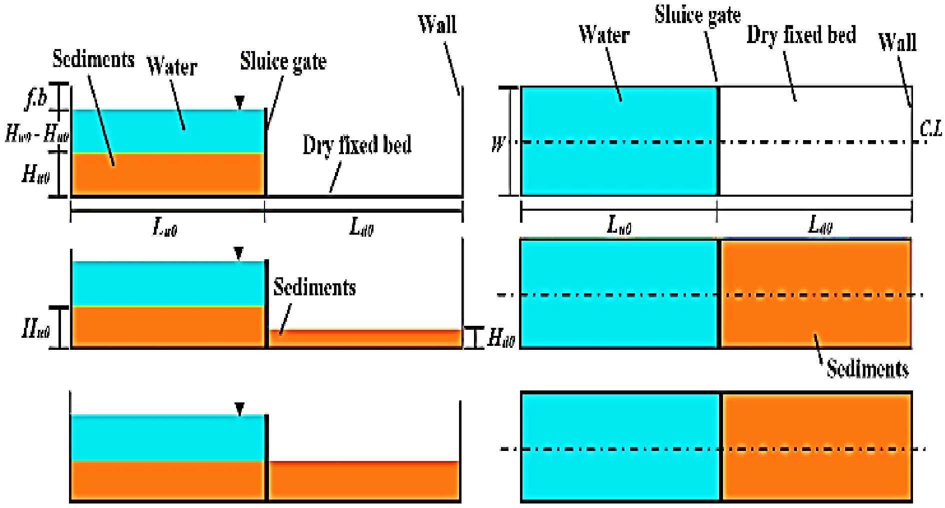

Figure (1). The configuration of the dam-break over mobile bed models (current study)

Materials and Methods

The dam-break flow characteristics are scrutinized by following process: (i) tracking the free-surface by standard VOF method using Flow-3D package; (ii) calculation of fluid pressure by implicit method; (iii) simulating the turbulent flow through the standard k-ε model; (iv) evaluation the bed-load transport using van Rijn formula.

Results

The sensitivity analysis was carried out on the cells mean diameter dm as well as the turbulence closure models including standard k-ε, k-w and RNG. Therefore, the accuracy of models in prediction the free surface height was evaluated in dam-break over the fixed and mobile beds. The normal root mean squares NRMSE presents the mod-eling accuracy criteria.

Table (1). The NRMSE of the mesh cells mean diameter in Lobovsky et al. (2014) experiment

	model A: 12.5-10				model B: 25-20			
duration of the dam-break t (s)	0.16	0.28	0.37	0.45	0.16	0.28	0.37	0.45
NRMSE values	0.0385	0.0262	0.0995	0.0565	0.0375	0.0294	0.109	0.0545

Table (2). The NRMSE of the turbulence closure models in Lobovsky et al. (2014) experiment

duration of the dam-break t (s)	0.16	0.28	0.37	0.45
k-ε	0.0389	0.0329	0.0471	0.0639
k-w	0.0434	0.0322	0.0471	0.0813
RNG	0.0434	0.0329	0.0471	0.0813

Table (3). The NRMSE of the van Rijn formula in Spinewine (2005)

	model C	model D	model E
mean diameter of cells in mesh blocks 1-2	25-20	25-20	25-20
duration of the dam-break t (s)	1.25	1.25	1.25
Van Rijn formula	0.0445	0.0559	0.0596

In tables 1-3, NRMSE values between zero and 0.1, 0.1 and 0.2, 0.2 and 0.4 present perfect, proper and average fit between the experimental and computational results, respectively. Therefore, the model performance in predicting the water free surface evolution is perfect in all cases. However, the computational efforts along with the accuracy in d0 = 25mm and standard k- ε closure model are lesser and higher than the other cases, respectively. Further, the van Rijn (1984) formula shows high performance in prediction the dam-break over the mobile bed (Table 3).

Indeed, according to fig. 1 where the bed elevation in the downstream is equal to zero, then rs = 0. Meanwhile, where the bed elevation through the downstream is equal to upstream (Hd0 = Hu0), then rs = 1. Whilst the free surface propagation and the bed deformation during the dam-break process are according to the figs. 2&3. In all modeling, the mean size of the mesh cells in both sand and pumice models is 25 mm. Further, the dam-break duration is equal to the tm = 10s.

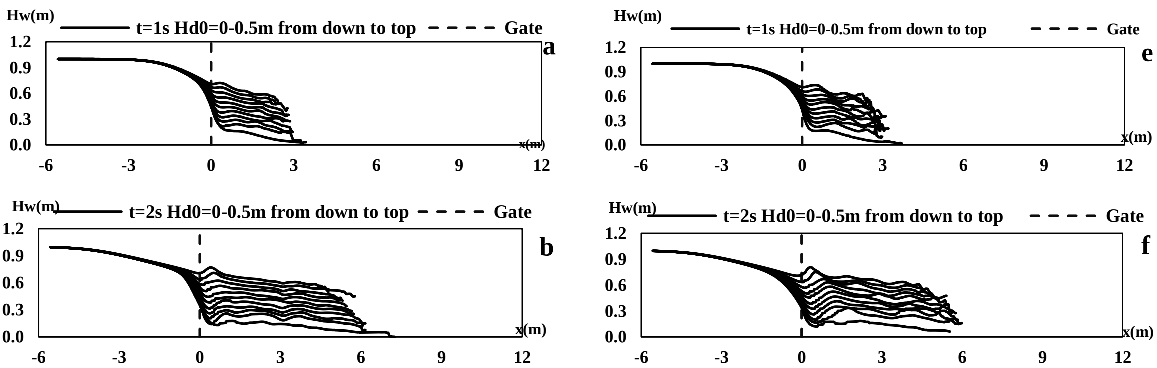

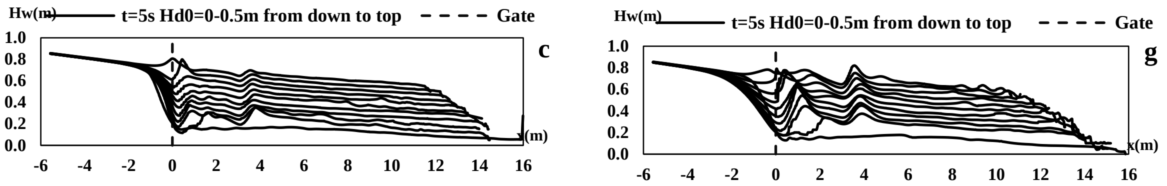

Figure (2). Evolution of free-surface profiles of sand (a-c) and pumice (e-g) at times t = 1s-5s, respectively

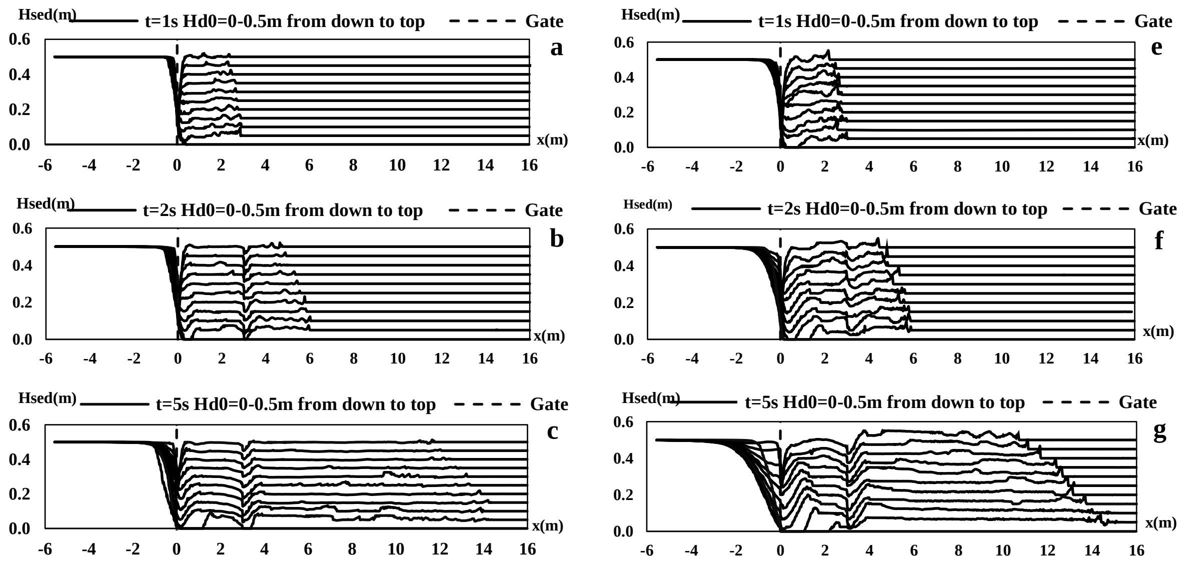

Figure (3). The bed profiles of the sand models (a-c) and pumice models (e-g) at times t = 1s-5s, respectively

Discussion

Considering figs. 2a-2g, increasing the rs value causes rising the wave front advancing distance. In figs. 2a & 2b, an increase in the rs value leads to rising the free-surface height H_w in the downstream near field. The H_{wmax} and H_{wmin} are corresponding to the r_s = 1 and r_s = 0, respectively. The profiles are parallel to each other while the free-surface has a steep gradient in the near field. In this regard, the pressure distribution changes from hydrostatics to hydrodynamics, from the flume beginning to the near field, respectively. The result is consistent with Stansby et al. (1998). In fig. 4c, two hydraulic jumps are formed in the near field and at the downstream except in the case r = 0. These are displaced to the upstream during the middle to the last stages (t = 5s – 7s). The result is consistent with Capart and Young (1998). They showed hydraulic jumps are generated across the downstream channel because of dam-break flow and the mobile bed interaction. However, in the current study, two hydraulic jumps are formed duo to flume considerable length as well as bed resistance that is intensified by scouring (Nsom et al. (2000)., Nsom et al. (2007)., Nsom et al. 2019., Khoshkonesh et al. (2019)., Heydari and Khoshkonesh (2016)). According to Wu and Wang (2008), an increase in the downstream length leads to changing the sediment transport rate from the bed- to the suspended-load. However, in the current study, the sediments are transported mainly in the bed-load form, despite the considerable length of the downstream channel. Considering fig. 2e (pumice), similarly fig. 2a (sand), an increase in rs leads to rising and reducing the Hw and x_f values, respectively. A possible reason is higher mobility of pumice than the sand that causes more bed resistance effect against the wave front propagation. In fig. 2g, there is no water rising in r=0. Further, rising r_s values leads to increasing the height of the second hydraulic jump. The first hydraulic jump approximately disappears in the case r_s =1. While, reducing the r_s value leads to decreasing the distance between the first and second hydraulic jumps. In fig. 2g, the greatest height of the first hydraulic jump (r_s = 0.3) is about $0.36H_{w0}$ and $0.75H_{u0}$, i.e., more than twice the fig. 2c. In figs. 2a-2g, the free-surface gradient is significant in the near field during the initial stages. Further, the free-surface has a steep slope near the straight line. Whereas, the gradient is modified due to increasing the reservoir releasing rate, during the middle to the last stages. Moreover, plunging the dam-break flow' kinematic energy causes an increase in viscosity effects. In fig. 3a, the bed scouring occurs significantly in the near field. In this region, the shear stress of the water flow exceeds the critical value of the bed. The result is consistent with Spinewine (2005). Moreover, rising the rs value results in reducing sediment transport in the far field. However, it leads to reducing the first scour hole width. Likewise, the sedimentation occurs in $0 < x < 3$m while its length is plunged with increment of the rs values. Indeed, there is a lag distance between the erosion and sedimentation regions due to non-equilibrium sediment transport conditions (Capart and Young (1998)., Fraccarollo and Capart (2002)). Fig. 3b illustrates the second scour hole emerges in $x \approx 3$m. It should be noted that the positions of both scour holes are at a short distance from the hydraulic jumps. Indeed, the resistance of the bed against the advancing the dam-break flow is the main reason for the formation of the hydraulic jumps. The result is not reported in previous studies (Capart and Young (1998)., Cao et al. (2004)., Wu and Wang (2008)). Whereas, increasing the r_s value leads to reducing the first hole width. The maximum width belongs to the case r_s =0.1. Further, the position of the second hole is not changed, despite increasing the rs. The greatest sedimentation occurs in the wave-front tip region. It's consistent with Cao et al. (2004). In figs 3b-3g the dimensions of the scour holes are considerably increased during the initial to the middle stages (t_m = 1-5s). As well, the highest and least unevenness of the bed profiles belong to r_s = 0.1 and r_s = 1 respectively. Consequently, in figs 3b – 3g, the complete bed scouring occurs in first and second holes, in case r_s = 0.1. Indeed, the flow capacity in eroding the bed is increased during the initial to the last stages. In fig. 3e (pumice), the dimensions of the first hole, the unevenness of the bed, the sedimentation rate in the wave-front tip region and the elevation of the sheet-flow profile are greater than the fig. 3a (sand). In fig. 3f, the second hole is less symmetrical relative to the fig. 3c. Besides, the dimensions of both holes are greater than the fig, 3c.

Conclusions

The modeling results showed: rising the downstream bed elevation leads to a) increas-ing the water free-surface height in the downstream, b) reducing the wave front ad-vancing distance to the downstream and rising water over the end-wall c) reducing the reservoir releasing rate. Two hydraulic jumps are formed at the downstream of the dam in all cases except the downstream with fixed-bed. Ultimately, it's concluded that the VOF along with the k-ε closure model, have high accuracy in predicting the characteristics of the dam-break flow over mobile beds.

References

Ahadiyan, J., Adeli, A., Bahmanpouri, F., Gualtieri, C., Khoshkonesh, A. (2021). Riprap ef-fect on hydraulic fracturing process of cohesive and non-cohesive coastal protective levees. *Water Resource Management*.

Bahmanpouri, F., Daliri, M., Khoshkonesh, A., Montazeri Namin, M., Buccino, M. (2020). Bed compaction effect on dam break flow over erodible bed; experimental and numerical modeling. Journal of Hydrology, 125645.

Banejad, H., Heydari, M., Khoshkonesh, A. (2015). The comparison of the performance of single-equation models of turbulence kinetic energy and two k-e equation models in hydrau-lic simulation of dam failure on the mobile bed. *International Conference on Modern Re-search in Agricultural Science and Environment, December 15th, Malaysia, Kuala Lumpur*

Cao, Z., Pender, G., Wallis, S., Carling, P. (2004). Computational Dam-Break Hydraulics over Erodible Sediment Bed. *J. Hydraul. Eng*. 130, 689–703.

Capart, H., Young, D.L. (1998). Formation of a jump by the dam-break wave over a granular bed. *J. Fluid Mech*. 372, 165–187.

Fraccarollo, L., Capart, H. (2002). Riemann wave description of erosional dam-break flows. *J. Flu-id Mech*. 461, 183–228.

Heydari, M., Khoshkonesh, A. (2016). The Comparison of the Performance of Prandtl | Mixing Length , Turbulence Kinetic Energy

, K-e , RNG and LES Turbulence Models in Simulation of the Positive Wave Motion Caused by Dam Break on the Erodible Bed. *Indian Journal of Science and Technology*. 9(7):1-33,87856. http://doi.org/ 10.17485/ijst/2016/v9i7/87856.

Khoshkonesh, A., Nsom, B., Bahmanpouri, F., Ahmadi Dehrashid, F., Adeli, A. (2021). Numerical study the dynamic and structure of partial dam-break flow using VOF method. Water Resource Management.

Khoshkonesh, A., Nsom, B., Gohari, S. and Banejad, H. (2019). A comprehensive study on dam break flow over dry and wet beds. *Ocean Engineering*, 188:106279.

Khoshkonesh, A., Gohari, S. and Banejad, H. (2019). Numerical Study of the effect of the flood-plain obstacles on dam-break flow by MPS method. *Journal of Water and Soil Conservation*. 26(6): 119-138. http://doi.org/ 10.22069/JWSC.2019.16153.3141.

Khoshkonesh, A., Nsom, B., Ahmadi Dehrashid, F., Heidarian, P., Riaz, Kh. (2021). Com-parison of the SWE and 3D models in simulation of the dam-break flow over the mobile bed. *5th the scientific conference of applied research in science and technology of Iran. Sep-tember 5th 2021.*

Khoshkonesh, A., Gohari, S. and Banejad, H., Ahmadi Dehrashid, F., Bajelvand, S. (2020). Kinematic analysis of dam-break flow over granular beds. *National Conference on Water Technology Development, Watershed Management and River Engineering, March 5th , Tehran University, Tehran.*

Nsom, B., Debiane, K., Piau, J.M. (2000). Bed slope effect on the dam break problem. *J. Hydraul. Res. 38.*

Nsom, B., Jenny, M., Askoura, Y., Peron, F. (2007). Numerical Solution to Horizontal Zero- iner-tia , Viscous Dam-Break Problem. *Innov. Adv. Tech. Comput. Inf. Sci. Eng*. 123–128.

Nsom, B., Latrache, N., Ramifidisoa, L., Khoshkonesh, A. (2019). Analytical Solution to the Stabil-ity of Gravity-driven Stratified Flow of Two Liquids over an Inclined Plane, in: *24th French Mechanics Congress in Brest. Brest*, p. 244178.

Spinewine, B. (2005). Two-layer flow behaviour and the effects of granular dilatancy in dam-break induced sheet-flow. *Université catholique de Louvain* (Belgium).

Stansby, P.K., Chegini, A., Barnes, T.C.D. (1998). The initial stages of dam-break flow. *J. Fluid Mech.*

Wu, W., Wang, S. (2008). One-Dimensional Modeling of Dam-Break Flow over Movable Beds. *J. Hydraul. Eng*. 133, 48–58.